

Magic-Boost: Boost 3D Generation with Mutli-View Conditioned Diffusion

Fan Yang¹ Jianfeng Zhang^{†2} Yichun Shi² Bowen Chen² Chenxu Zhang²
Huichao Zhang² Xiaofeng Yang¹ Jiashi Feng² Guosheng Lin^{†1}

¹ Nanyang Technological University
² ByteDance Inc.



Fig. 1: Provided with an input image and its coarse 3D generation, MagicBoost effectively boosts it to a high-quality 3D asset within 15 minutes. From left to right, we show the input image, pseudo multi-view images and coarse 3D results from Instant3D, together with the significantly improved results produced by our method.

Abstract. Benefiting from the rapid development of 2D diffusion models, 3D content creation has made significant progress recently. One promising solution involves the fine-tuning of pre-trained 2D diffusion models to harness their capacity for producing multi-view images, which are then lifted into accurate 3D models via methods like fast-NeRFs or large reconstruction models. However, as inconsistency still exists and limited generated resolution, the generation results of such methods still

[†]Corresponding author.

lack intricate textures and complex geometries. To solve this problem, we propose Magic-Boost, a multi-view conditioned diffusion model that significantly refines coarse generative results through a brief period of SDS optimization ($\sim 15\text{min}$). Compared to the previous text or single image based diffusion models, Magic-Boost exhibits a robust capability to generate images with high consistency from pseudo synthesized multi-view images. It provides precise SDS guidance that well aligns with the identity of the input images, enriching the local detail in both geometry and texture of the initial generative results. Extensive experiments show Magic-Boost greatly enhances the coarse inputs and generates high-quality 3D assets with rich geometric and textural details [project page](#).

1 Introduction

The recent surge in the development of 2D diffusion models has unlocked new prospects for 3D content generation. A particularly viable strategy involves fine-tuning pre-trained 2D diffusion models to catalyze their capacity for generating images with multi-view consistency, which are then lifted to accurate 3D models through fast-NerFs or large reconstruction models [13, 17, 19, 20]. For example, Instant3D [13] firstly finetune the pre-trained 2D diffusion models to unlock the ability of multi-view image generation, and then utilize a robust reconstruction model to derive 3D representations; Wonder3D [19] finetunes the 2D diffusion model with cross-domain attention layers to enhance the 3D consistency of generative outputs. Despite the efficiency of these methods in producing 3D assets from textual prompts or images, the generated results are still coarse, characterized by a lack of fine textures and complex geometries. This is primarily caused by local inconsistencies and the limited resolution of the generative process.

A potential solution is to enhance the generated results of such methods with Score Distillation Sampling (SDS) optimization [5, 18]. Commencing with a coarse 3D model, efforts have been made to refine it through SDS optimization with small noise levels, utilizing text or single-view conditioned diffusion models [16, 26]. However, we argue that both text and single-view image conditions are inadequate in providing explicit control and precise guidance. This inadequacy often results in identity shifts, blurred textures, and geometric inaccuracies. Specifically, the inherent ambiguity of textual descriptions poses a challenge for text-conditioned diffusion models, such as StableDiffusion and DeepFoldy-IF, to maintain a consistent identity throughout the optimization process. Consequently, the optimized results may diverge significantly from the initial models, potentially defying users' expectations. Single-view image-guided diffusion models like Zero-1-to-3 [16] endow 2D diffusion models with the capacity for viewpoint conditioning. Nevertheless, constrained by the limited information provided by single-view inputs, Zero-1-to-3 and subsequent methods [3, 16, 17, 19, 30, 41] are prone to generating unpredictable and implausible shapes and textures during novel view prediction or SDS optimization, leading to flattened geometries and blurry textures.

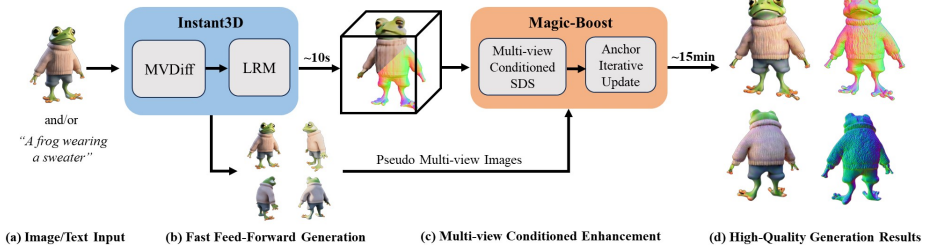


Fig. 2: The overall pipeline. We build MagicBoost with Instant3D [13] (a synergy of Multi-view Diffusion (MVDiff) and Large Reconstruction Model (LRM)), which provides pseudo multi-view images together with a coarse 3D output. Conditioned on the generated multi-view inputs, our model provides precise SDS guidance, thereby significantly augmenting the coarse 3D outputs within a brief interval (~ 15 min).

To tackle the challenges in refining coarse 3D generations, we present MagicBoost, a multi-view conditioned diffusion model that ingests multi-view images as inputs, implicitly encoding 3D information across different views. MagicBoost exhibits a robust capability to generate images with high 3D consistency as well as provide precise SDS guidance that aligns well with the identity of the input images, enriching the local detail in both geometry and texture of the initial generated results. Built upon the Stable Diffusion architecture, we introduce an advanced method to efficiently distill dense local features from multi-view inputs with a denoising U-Net operating at a fixed time step. In line with prior arts [19, 31, 34], our model employs a self-attention mechanism to enable interactions and information sharing across different views, thus implicitly encoding the multi-view correlations. However, relying exclusively on ground-truth multi-view images for training produces unsatisfying results. We meticulously develop a series of data augmentation strategies, including random drop, random scale, and noise disturbance, to facilitate the training process, leading to more robust performance. We also introduce a condition label that allows users to manually adjust the influence of different input views, strength the influence of high-fidelity input views while mitigating that of lower-quality ones. To further enhance the optimization process, we present a novel Anchor Iterative Update loss to address the over-saturation problem in SDS, culminating in the generation of high-quality content with realistic textures.

As shown in Fig. 2, our testing framework integrates Instant3D [13], a two-stage feed-forward generative approach, which firstly generates four multi-view images with finetuned 2D diffusion models, followed by the utilization of a large reconstruction model for 3D reconstruction. Given the four synthesized multi-view images from Instant3D as inputs, our model is capable of synthesizing highly consistent novel views and provides precise SDS guidance, refining the coarse generated results within a short time period (~ 15 min). Comprehensive evaluations demonstrate MagicBoost substantially enhances the quality of

coarse inputs, efficiently yielding 3D assets of better quality with intricate geometries and authentic textures, as shown in Fig. 1.

2 Related Works

3D generation Models. Traditional GAN-based methods explore generation of 3D models with different 3D representations including voxels [10, 32], point clouds [1, 38] and meshes [7, 37]. These methods, predominantly trained on limited-scale 3D datasets, often fall short in generating intricate geometric structures with substantial diversity. The advent of diffusion models in 2D generative tasks has prompted several explorations into their application within 3D domains, training diffusion models directly on 3D datasets. For example, Shape [11] trains an conditional diffusion models by encoding each 3D shape into a set of parameters of an implicit function. Nonetheless, the generative quality of such methods remains constrained by the scarce availability and variety of 3D datasets. Even though the largest 3D dataset [4] in recent years are still much smaller than the datasets used for 2D image generation training [29]. Recently, a novel paradigm has emerged for 3D generation that circumvents the need for large-scale 3D datasets by leveraging pretrained 2D generative models. Leveraging the semantic understanding and high-quality generation capabilities of pretrained 2D diffusion model, Dreamfusion [25], for the first time, propose to optimize 3D representations directly with 2D diffusion model utilizing the Score distilling Sampling loss. Followoing works [2, 15, 26, 39] continue to enhance various aspects such as generation fidelity and training stability by proposing different variations of SDS such as VSD [35]. Although being able to generate high-quality 3D contents, these methods suffer from extremely long time for optimization, which greatly hinders its application in the real-world scenario. Another line of works try to finetune the pretrained 2D diffusion network to unlock its ability of generating multi-view images simultaneously, which are subsequently lifted to 3D models with fast-NeRF [24] or large reconstruction models [13, 17, 19, 20]. Although these methods generates reasonable results, they are still limited by the local inconsistency and limited generation resolution, producing coarse results without detailed textures and complicated geometries.

Novel View Synthesis. The success of diffusion model on the 2D task has opened a new door for the task of zero-shot novel view synthesis. Finetuned on Stable Diffusion, Zero-1-to-3 [16] achieves viewpoint-conditioned image synthesis of an object from a single in-the-wild. Subsequent [17, 30, 41] works further improves the generative quality by refining network architectures and optimizing training methodologies. Yet, constrained by the limited scope of single-view input, these models encounter challenges in producing accurate novel views with robust 3D consistency. In contrast, EscherNet [12] propose to learn implicit and generative 3D representations coupled with specialised camera positional encodings, allowing the network to fuse information from arbitrary number of reference and target views, which greatly improves the 3D understanding of the network, leading to better generation results. In parallel with EscherNet, our model also

employs multi-view inputs to enhance the accuracy of the 3D generation. However, we operate within a more challenging task—enhancing the local details of the coarse 3D model with generated pseudo multi-view images as inputs.

3 Methods

Given a coarse 3D asset and its corresponding multi-view generated pseudo images, we aim to improve the asset’s quality, enriching both geometry and texture through SDS optimization within a short time period. To achieve this, we propose Magic-Boost, a diffusion model conditioned on multiple views that adeptly encodes 3D information and ensures multi-view consistency. This model is designed to provide precise SDS guidance, thereby refining the local details of the initial coarse results. Magic-Boost is built upon the Stable Diffusion architecture, where we adeptly extract dense local features via a denoising U-Net operating at a fixed timestep and adopt the self-attention mechanism to facilitate interactions and information exchange across different views, as detailed in Sec. 3.1. To enhance the training process, we introduce several data augmentation strategies, as elaborated in Sec. 3.2. Our testing framework is built on Instant3D. In the refinement phase, we introduce an Anchor Iterative Update loss to alleviate the over-saturation problem of SDS, leading to high-quality generation results with detailed geometry and realistic textures, as presented in Sec. 3.3.

3.1 Multi-view Conditioned Diffusion

Formulation. Given n views $v_0, v_1, \dots, v_n \in \mathbb{R}^{H \times W \times 3}$, each capturing an object from a distinct perspective with relative angles $\Delta\gamma_0 = 0, \Delta\gamma_1, \dots, \Delta\gamma_n$ of an object as input, the objective of our multi-view conditioned diffusion model is to synthesize a novel view x at a relative angle $\Delta\gamma_x$. To this end, we compute the camera rotation $R_i \in \mathbb{R}^{3 \times 3}$ and translation $T_i \in \mathbb{R}^3$ corresponding to each relative angle $\Delta\gamma_i, i \in (0, 1, \dots, n, x)$ and subsequently train the model \mathcal{M} to generate the novel view x . The relative camera pose is denoted as $c_i = (R_i, T_i), i \in (0, 1, \dots, n, x)$, and the formulation of our model is as follows:

$$x_{c_x} = \mathcal{M}(v_0, \dots, v_n, c_0, \dots, c_n, c_x) \quad (1)$$

In our experiments, we follow the setting of Instant3D and employing a four-view arrangement, where the four condition views are orthogonal to each other with relative angles set at $\Delta\gamma_0 = 0, \Delta\gamma_1 = 90, \Delta\gamma_2 = 180$, and $\Delta\gamma_3 = 270$.

Image Feature Extractor. To synthesize consistent novel views, it’s crucial to capture both the global features with high-level semantics, and the local features with dense local details.

Global Feature Extractor. In line with previous works [16, 23, 34, 40], we utilize a frozen CLIP pre-trained Vision Transformer (ViT) [27] to encode high-level signals, which provide global control on the generated images. However, as CLIP encodes images into a highly compressed feature space, we found that encoding

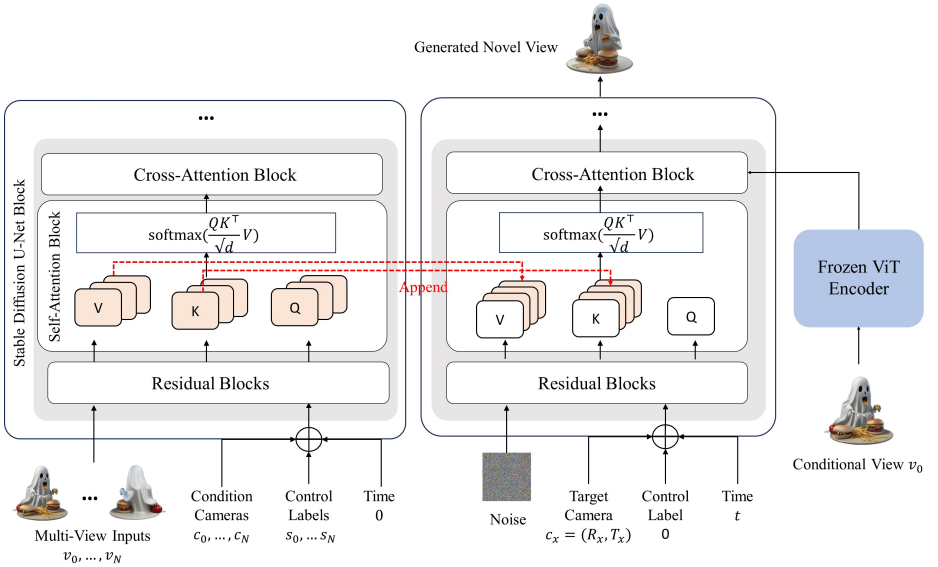


Fig. 3: Architecture of our multi-view conditioned diffusion model. At the core of our model lies the extraction of dense local features facilitated by a denoising U-Net operating at a fixed timestep. Concurrently, we harness a frozen CLIP ViT encoder to distill high-level signals. The original 2D self-attention layer is extended into 3D by concatenating keys and values across various views. To further control the condition strength of different views, we involve a condition label which allows users to manually control the condition strength of different input views independently.

the global feature of only the first input view (where $\gamma_0 = 0$) is sufficient to generate satisfactory results, while encoding multi-view global features does not lead to improvement on the performance. Consequently, we only encode the global feature of the first input view in our experiments.

Local Feature Extractor. Multi-view images provide dense local details, pivotal for novel view synthesis. However, accurately and efficiently encoding local dense features from multi-view inputs is non-trivial. Zero-1-to-3 [16] attempts to encode dense local signals by appending the reference image to the input of the denoising U-Net within Stable Diffusion. This approach, however, enforces an misaligned pixel-wise spatial correspondence between the input and target images. Zero123++ [30] extracts local feature by processing an additional reference image through the denoising U-Net model. It synchronizes the Gaussian noise level of the input images with that of the denoising input, enabling the U-Net to focus on pertinent features at varying noise levels. While this method is adept at extracting dense local features, it leads to much more computational costs, by extracting different feature maps at each denoising step. To address this issue, we propose a novel technique that extracts dense local features using the denoising U-Net at a fixed timestep. Specifically, we employ the denoising U-Net

to extract low-level features from clean images without introducing any noise, and we consistently set the timestep to zero. This approach not only captures features with dense local details but also significantly accelerates the generation process by extracting local features just once throughout the entire optimization or diffusion procedure.

Multi-view Conditioned Generation. The overall architecture of our model is shown in Fig. 3. Our multi-view conditioned diffusion model is built on Stable Diffusion backbone. We incorporate global features via the cross-attention module, following methods such as IP-Adapter [40] and ImageDream [34]. The denoising U-Net, operating at a fixed timestep, is harnessed to distill dense local features from multi-view inputs. These features are subsequently integrated into the self-attention module to encode 3D correspondence. Similar with prior arts [19, 31], we extend the original 2D self-attention layer of Stable Diffusion into 3D by concatenating the keys and values of different views within the self-attention layers, which facilitates the interactions across different input views and implicitly encodes multi-view correspondence. Additionally, camera poses are injected into the denoising U-Net for both the conditional multi-view inputs and the target view. Specifically, a two-layer MLP is employed to encode camera poses into one-dimensional embeddings, which are then added to time embeddings as residuals.

3.2 Data Augmentation

We train the multi-view conditioned diffusion model with ground-truth multi-view images rendered from Objaverse [4]. However, directly training with these ground-truth images can lead to suboptimal results during inference, as the domain discrepancy between the ground-truth multi-view images and the synthesized ones used during testing engenders artifacts and inconsistent generative results. Moreover, when trained with multi-view images, the model may develop a bias towards the nearest anchor view, neglecting information from other views, which can result in inaccurate outputs that fail to maintain 3D consistency

To solve these problems, we propose several data augmentations strategies to enhance the training process and ensuring robust performance:

- *Noise Disturb and Random Scale:* To emulate the blurry textures and local inconsistencies present in synthesized multi-view images, we introduce noise disturb augmentation, which perturbs the conditional multi-view images with Gaussian noise sampled at different timesteps. This is coupled with random scale augmentation, employing a downsample-and-upsample approach to generate blurry training inputs, thereby enhancing the model’s capability to handle such imperfections.
- *Random Drop:* To circumvent the model’s tendency to rely excessively on the nearest conditional view, we implement random drop augmentation. This technique randomly omits conditional views during training, enforcing the network to synthesize more consistent results by integrating information from all available views.

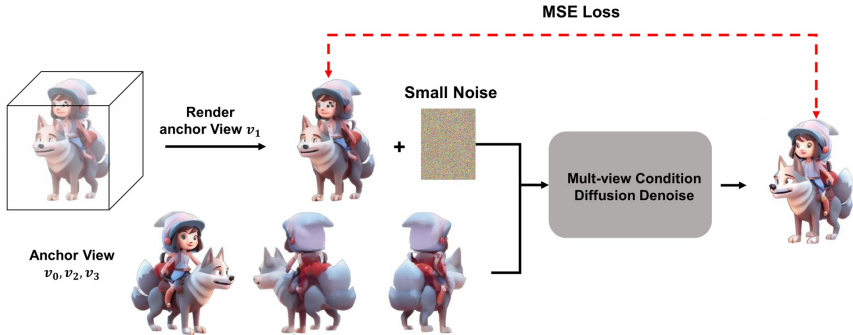


Fig. 4: Illustration of the anchor iterative update loss.

Similar as LGM [33], we also incorporate grid distortion to disrupt the 3D coherence of ground-truth images and camera jitter augmentation to vary the conditional camera poses of multi-view inputs.

To further control the influence of different views, we introduce a condition label enabling manual adjustment of the input views’ conditioning strength. This label, indicative of the conditional intensity, is processed by a two-layer MLP into a one-dimensional vector, which is then combined with the time embedding in the local feature extractor to guide the generation process. For the target view, the condition label is consistently zero. This condition label is concurrently trained with our data augmentation strategy. When employing more augmentation scales, such as noise perturbation with larger timesteps, we assign a higher value to the condition label to reduce the condition weights, and conversely for smaller scales.

3.3 Refinement with SDS Optimization

As shown in Fig. 2, We build our test pipeline with Instant3D [13], a two-stage feed-forward generation method which firstly generates four multi-view images with finetuned 2D diffusion networks and then lift the multi-view images to 3D model utilizing large reconstruction model. However, due to limited resolution and local inconsistency, the generated results are still in low quality without detailed texture and complicated geometry. Leveraging the generated pseudo multi-view as input, we propose to adopt SDS optimization with small noise level to further enhance the coarse generation results. Benefit from the high-fidelity geometry and texture information provided by the pseudo multi-view inputs, our model is capable of generating highly consistent novel views and providing precise SDS guidance to enhance the coarse generated results within a short time period (~ 15 min).

Specifically, we first convert the generated mesh from Instant3D into differentiable 3D representations by randomly rendering and distilling the appearance and occupancy of the mesh with L1 loss. In our experiments, This process is

achieved with a fast NeRF (e.g. InstantNGP [24]) with little time cost (~ 1 min). After initialization, we optimize the fast NeRF utilizing SDS loss with a small range of denoising timestep as $[0.02, 0.5]$. The optimization process takes about 15min with 2500 steps, which is much more efficient compared to the $1 \sim 2$ hours time cost of traditional SDS-based methods [25, 34, 35].

We further introduce an Anchor Iterative Update loss to alleviate the over-saturation problem of SDS optimization. Specifically, we draw inspiration from the recent image editing methods [9, 22] that edit the NeRF by alternatively rendering dataset image, updating the dataset and then supervising the NeRF reconstruction with the updated dataset images. In our generation task, we could also regard the input pseudo multi-view inputs as our initial anchor datasets and adopt a similar update strategy by first rendering anchor view image, perturbing the image with random noise and then apply a multi-step denoising process with the proposed multi-view condition diffusion model. However, as the denoising process is guided by the multi-view inputs themselves, simply adopt such as process leading to minor refinement on the input anchor images. To address this problem, while updating certain anchor view v_1 , we drop it in the condition inputs for the multi-view diffusion models, and denoise leveraging other views v_0, v_2, v_3 . We found this works well and achieve accurate refinement on the local details of the anchor image, while preserving the 3D consistency. The refined anchor image is then used to supervise the generation with MSE loss, as illustrated in Fig. 4. As shown in the bottom line of Fig. 7, the proposed Anchor Iterative Update loss alleviates the over-saturation problem and generates realistic textures, leading to better generation performance.

4 Experiments

4.1 Implementation Details

Datasets. We train our model on the public available Objaverse [4] dataset which contains around 800k 3D objects. After adopting simple filter leveraging CLIP [27] to remove the objects whose rendered images are not relevant to its name, we have about 350K objects at the end. For each object, we randomly pick two elevation angles and render 32 images with the azimuth evenly distributed in $[0^\circ, 360^\circ]$. We then follow the setting of MVDream [31] to render multi-view RGB images for training.

Training. We train our model on 32 NVIDIA V100 GPUs for 30k steps with batchsize 512. The total training process cost about 6 days. We use 256×256 as the image resolution for training. For each batch we randomly sample 4 views as conditional multi-view images and another one view as the target view. The model is initialized from MVDream (the version of stable diffusion 2.1) and the optimizer settings and ϵ -prediction strategy are retained from the previous finetuning except we reduce the learning rate to $1e-5$ and use 10 times learning rate for camera encoders' parameters for faster convergence. As there is no official code for instant3D [13], we reproduce it follows the published paper and use it as our base model to generate the pseudo multi-view images and the coarse



Fig. 5: Qualitative Comparison between our method with others.

initial shape. (More implementation details could be found in the Supplementary Materials).

4.2 Qualitative Comparisons.

We make comparisons with State-Of-the-Art methods on Image-to-3D generation, including Zero123-XL [16] and ImageDream [34]. As shown in Fig. 5, our method generates visually better results with sharper textures, better geometry and highly consistent 3D alignment. Zero-1-to-3 [16] empowers 2D diffusion models with viewpoint conditioning, enabling zero-shot novel view synthesis conditioned on a single-view image. However, limited by the incomplete information provided by a single-view input, it suffers from high uncertainty on the occluded regions, struggling to generate the unseen regions with implausible shapes and chaotic texture. Compared to Zero123, our model benefits from more comprehensive information obtained from the multi-view inputs, migrating the problems of flat geometry and blurry textures and generates high-quality results. ImageDream [34] extends MVDream [31] to start from a given input image, which proposes a new variant of image conditioning. Compared to Zero-1-to-3, ImageDream employs self-attention to establish multi-view correspondence,

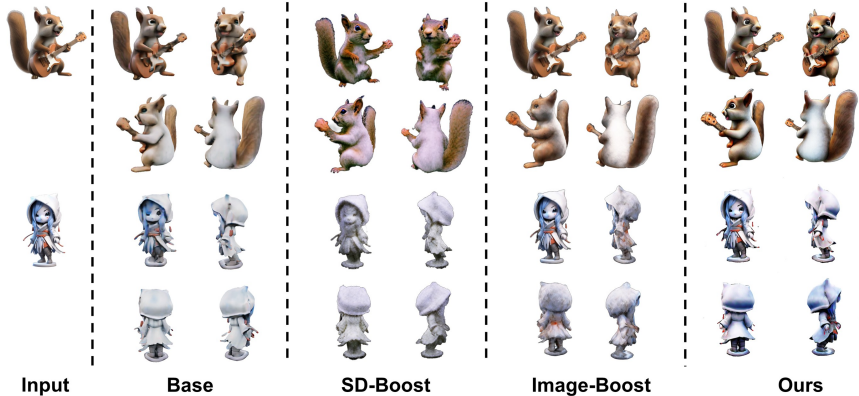


Fig. 6: Qualitative comparison between our method with other refinement methods. From left to right, we show input, followed by the initial results from instant3D [13], and culminates with the results derived from StableDiffusion Boost, Zero123-XL [16] Boost, and our multi-view conditioned model.

generating more accurate shapes. However, as shown in Fig. 5, it still generates results with over-saturated colors and over-smooth textures. Comparison to Imagedream, our model benefits from much stronger and more precise constraints provided by the pseudo multi-view inputs, leading to higher generation quality with photo-realistic colors and more geometric details.

We also make comparisons by using other diffusion models at the optimization stage to boost the coarse results, including Stable Diffusion and Zero123-XL [16]. Note we only compare with methods that supports or built on relative camera coordinates. As ImageDream [34] is trained in its own camera canonical space, it could not be used in the boost stage directly. For the fairness, we replace our multi-view conditioned diffusion model with other diffusion models at the boost stage while keeping other settings unchanged. As shown in Fig. 6 and Tab. 1, limited by the ambiguity of text description, Stable Diffusion fails to keep the identity of the initiated coarse object fixed while changing it into another one with different texture and incorrect geometry. Although empowered with single-view image input in the cross-attention to synthesize novel views, Zero123-xl still lacks the ability to generate accurate 3D contents with consistent geometry and detailed texture, especially for the unseen regions. As shown in Fig. 6, it fails to enhance the occluded regions of the initial objects and generates 3D inconsistent texture with even lower qualities. Compared to these methods, our model acquires strong ability of generating highly consistent images from the pseudo multi-view images and provides more precise SDS guidance which can effectively maintain the identity and enhance local details in both geometry and texture of initial generation results.

Table 1: Quantitative Comparisons with image-to-3D methods.

Model	QIS	CLIP(TX)	CLIP(IM)	Time
MVDream	27.42 ± 4.92	31.42 ± 3.34	79.36 ± 4.20	~ 1h
Zero123-XL [16]	27.92 ± 2.41	29.11 ± 3.65	79.48 ± 6.73	~ 10min
Magic123 [26]	25.12 ± 4.29	29.31 ± 4.69	82.92 ± 9.33	~ 1h
ImageDream [34]	25.86 ± 3.68	31.53 ± 3.30	83.79 ± 4.25	~ 2h
Basemodel(Instant3D)	23.16 ± 2.53	30.61 ± 3.22	83.20 ± 5.45	~ 10s
SD-Boost	22.85 ± 4.37	30.26 ± 3.51	78.21 ± 10.32	~ 15min
Zero123-Boost	23.08 ± 3.31	29.67 ± 3.09	81.73 ± 5.96	~ 15min
MagicBoost (w/o Aug)	27.96 ± 3.22	31.43 ± 2.61	86.24 ± 4.66	~ 15min
MagicBoost (w/o AIU)	27.69 ± 3.51	31.50 ± 2.73	87.21 ± 4.43	~ 15min
MagicBoost	27.81 ± 3.81	31.57 ± 2.71	87.30 ± 4.45	~ 15min

4.3 Quantitative Comparisons.

Following ImageDream [34], we adopt three metrics for quantitative comparison of our methods with others, including the Quality-only Inception Score [28] (QIS) and CLIP [27] scores that calculated with text prompts and image prompts, respectively. Among which, QIS evaluates image quality and CLIP scores assess the coherence between the generated models and the prompts. The evaluation dataset consists of 37 high-resolution images, which is generated by SDXL with well-curated prompts. We present the quantitative comparison results in Tab. 1. As shown in the results, our model achieves higher scores on all the three metrics compared to other method, demonstrating the great image conditioned generation ability of our models. As the condition image is synthesized by text prompt, the highest CLIP-Text score also demonstrates the capability of our model to generates highly text-aligned contents. We also compare the inference time of different methods, which is calculated on a single A100 GPU. Notably, the inference speed of our model is significantly faster than the traditional optimization-based methods like Magic123 [26] and ImageDream [34], while achieving better generation quality.

4.4 Ablation Study.

Number of condition views. In the top row of Fig. 7, we show the effects of our multi-view conditioned diffusion model to synthesize novel views with different number of inputs. As illustrated in the Fig. 7, when there is only one single view input, our model fails to generate view consistently novel-view images. This demonstrates that the diffusion model struggle to acquires accurate 3D information from only one view input, resulting in the inconsistent generation results. However, as the number of the condition views increases, the generation fidelity of our model gradually increases, leading to more consistent

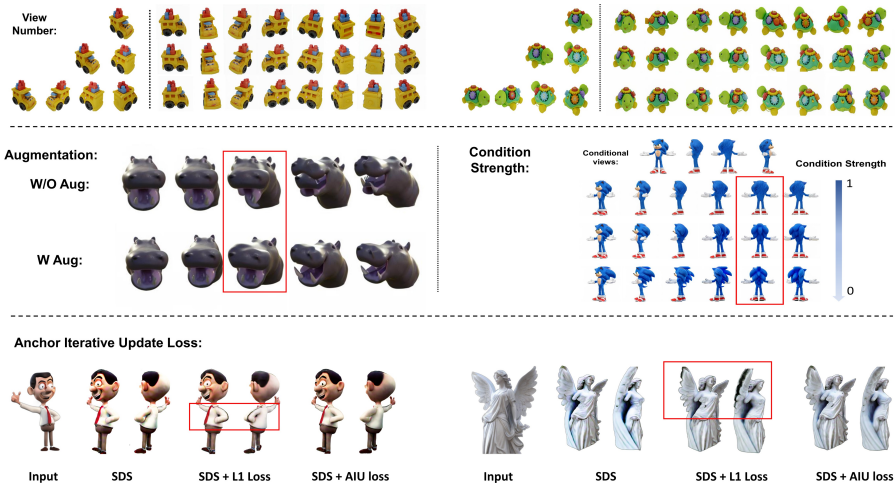


Fig. 7: Ablation Studies, including number of condition views, data augmentation, Anchor Iterative Update loss.

results which demonstrates the necessity of our proposed multi-view conditioned diffusion model.

Data augmentation. We compare models trained with/without data augmentation in Tab. 1 and Fig. 7. As shown in the left figure of Fig. 7, model trained without data augment fails to generate 3D consistent results as a result of learning strong condition to certain nearest anchor view while ignoring information from others. In comparison, with the proposed data augmentation strategy, our model learns to fuse the information from all conditional views and generate highly consistent 3D results. Another advantage of our model is to use the condition strength to control the condition strength of each input view, which allows user to strength the influence of high-quality views while weaken the ones with 3D inconsistency or in low-quality. As illustrated in the middle of Fig. 7, by fixing the weights of the first input view while lowing the weights of others, the model learns to generate diverse realistic results without constraining strictly by the input views. By setting the condition strength at different level, our model is capable to deal with inputs in different quality level, which improves the robustness of our model. (Please refer to the supplementary materials for more qualitative results.)

Anchor Iterative Update loss. We adopt Anchor Iterative Update loss to deal with the over-saturation problem of SDS. However, a more straightforward method is to simply use L1 loss from four pseudo multi-view images to constrain the appearance of the object from being away from the input. However, as illustrated in the bottom line of Fig. 7, L1 loss highly rely on the consistency of the input multi-view images, leading to obvious artifacts with collapsed textures at the inconsistent regions between different views. Instead, Anchor Iterative Update loss, leveraging the iterative render, update and distill strategy, alleviates



Fig. 8: Comparison with generation from scratch. Given the coarse 3D model as initialization, our model is capable to generate high-quality results comparable to those generating from scratch, which takes $\times 5$ time ($\sim 1.2\text{h}$), emphasizing the effectiveness of our overall pipeline.

the over-saturation problem by gradually distilling the clean RGB image refined from the updated rendered anchor images, leading to more robust performance with realistic appearance.

Generation with coarse initialization. In addition, we evaluated the impact of utilizing the coarse reconstruction outcomes obtained from a larger reconstruction model as an initialization step. As illustrates in Fig. 8, when provided with pseudo multi-view inputs, our model is capable of producing high-quality 3D contents from scratch. However, this process requires approximately $\times 5$ time (1.2h) for our model to achieve comparable results to those generated using the coarse reconstruction outputs as initialization. This result emphasizes the effectiveness of our overall approach.

5 Limitation.

Our model can effectively generate high-quality outputs, but its performance is still limited by the following factors: 1) The use of pseudo 3D multi-view images synthesized by the finetuned 2D multi-view diffusion model as inputs imposes an unavoidable influence on our model’s performance. Therefore, the generation quality of the multi-view diffusion model directly affects our model’s performance. Exploring 2D multi-view diffusion models with better generation quality would further improve our model’s performance. 2) Our model’s resolution 256×256 remains constrained in contrast to text-conditioned 2D diffusion models, which generate images with higher resolution containing more details. Uplifting our model to a higher resolution, such as 512×512 , would produce superior generation outcomes, allowing for more intricate geometry and detailed texture.

6 Conclusion

We present Magic-Boost, a multi-view conditioned diffusion model which takes pseudo generated multi-view images as input, implicitly encodes 3D information from different views, and capable of synthesising highly consistent novel view

images and providing precise SDS guidance during the optimization process. Extensive experiments demonstrate our model greatly enhances the generation quality of coarse input and generates high-quality 3D assets with detailed geometry and realistic texture within a short time period.

References

1. Achlioptas, P., Diamanti, O., Mitliagkas, I., Guibas, L.: Learning representations and generative models for 3d point clouds. In: International conference on machine learning. pp. 40–49. PMLR (2018) [4](#)
2. Chen, C., Yang, X., Yang, F., Feng, C., Fu, Z., Foo, C.S., Lin, G., Liu, F.: Sculpt3d: Multi-view consistent text-to-3d generation with sparse 3d prior. arXiv preprint arXiv:2403.09140 (2024) [4](#)
3. Chen, Y., Fang, J., Huang, Y., Yi, T., Zhang, X., Xie, L., Wang, X., Dai, W., Xiong, H., Tian, Q.: Cascade-zero123: One image to highly consistent 3d with self-prompted nearby views. arXiv preprint arXiv:2312.04424 (2023) [2](#)
4. Deitke, M., Schwenk, D., Salvador, J., Weihs, L., Michel, O., VanderBilt, E., Schmidt, L., Ehsani, K., Kembhavi, A., Farhadi, A.: Objaverse: A universe of annotated 3d objects. In: Proceedings of the IEEE/CVF Conference on Computer Vision and Pattern Recognition. pp. 13142–13153 (2023) [4](#), [7](#), [9](#)
5. Ding, L., Dong, S., Huang, Z., Wang, Z., Zhang, Y., Gong, K., Xu, D., Xue, T.: Text-to-3d generation with bidirectional diffusion using both 2d and 3d priors. arXiv preprint arXiv:2312.04963 (2023) [2](#)
6. Downs, L., Francis, A., Koenig, N., Kinman, B., Hickman, R., Reymann, K., McHugh, T.B., Vanhoucke, V.: Google scanned objects: A high-quality dataset of 3d scanned household items. In: 2022 International Conference on Robotics and Automation (ICRA). pp. 2553–2560. IEEE (2022) [18](#), [19](#)
7. Gao, L., Yang, J., Wu, T., Yuan, Y.J., Fu, H., Lai, Y.K., Zhang, H.: Sdm-net: Deep generative network for structured deformable mesh. ACM Transactions on Graphics (TOG) **38**(6), 1–15 (2019) [4](#)
8. Guo, Y.C., Liu, Y.T., Shao, R., Laforte, C., Voleti, V., Luo, G., Chen, C.H., Zou, Z.X., Wang, C., Cao, Y.P., et al.: threestudio: A unified framework for 3d content generation. threestudio: A unified framework for 3d content generation (2023) [18](#)
9. Haque, A., Tancik, M., Efros, A.A., Holynski, A., Kanazawa, A.: Instruct-nerf2nerf: Editing 3d scenes with instructions. arXiv preprint arXiv:2303.12789 (2023) [9](#)
10. Henzler, P., Mitra, N.J., Ritschel, T.: Escaping plato’s cave: 3d shape from adversarial rendering. In: Proceedings of the IEEE/CVF International Conference on Computer Vision. pp. 9984–9993 (2019) [4](#)
11. Jun, H., Nichol, A.: Shap-e: Generating conditional 3d implicit functions. arXiv preprint arXiv:2305.02463 (2023) [4](#)
12. Kong, X., Liu, S., Lyu, X., Taher, M., Qi, X., Davison, A.J.: Eschnet: A generative model for scalable view synthesis. arXiv preprint arXiv:2402.03908 (2024) [4](#)
13. Li, J., Tan, H., Zhang, K., Xu, Z., Luan, F., Xu, Y., Hong, Y., Sunkavalli, K., Shakhnarovich, G., Bi, S.: Instant3d: Fast text-to-3d with sparse-view generation and large reconstruction model. arXiv preprint arXiv:2311.06214 (2023) [2](#), [3](#), [4](#), [8](#), [9](#), [11](#)
14. Li, S., Li, C., Zhu, W., Yu, B., Zhao, Y., Wan, C., You, H., Shi, H., Lin, Y.: Instant-3d: Instant neural radiance field training towards on-device ar/vr 3d reconstruction. In: Proceedings of the 50th Annual International Symposium on Computer Architecture. pp. 1–13 (2023) [18](#)

15. Lin, C.H., Gao, J., Tang, L., Takikawa, T., Zeng, X., Huang, X., Kreis, K., Fidler, S., Liu, M.Y., Lin, T.Y.: Magic3d: High-resolution text-to-3d content creation. In: Proceedings of the IEEE/CVF Conference on Computer Vision and Pattern Recognition. pp. 300–309 (2023) [4](#)
16. Liu, R., Wu, R., Van Hoorick, B., Tokmakov, P., Zakharov, S., Vondrick, C.: Zero-1-to-3: Zero-shot one image to 3d object. In: Proceedings of the IEEE/CVF International Conference on Computer Vision. pp. 9298–9309 (2023) [2](#), [4](#), [5](#), [6](#), [10](#), [11](#), [12](#), [19](#), [20](#), [25](#)
17. Liu, Y., Lin, C., Zeng, Z., Long, X., Liu, L., Komura, T., Wang, W.: Syncdreamer: Generating multiview-consistent images from a single-view image. arXiv preprint arXiv:2309.03453 (2023) [2](#), [4](#), [19](#)
18. Liu, Z., Li, Y., Lin, Y., Yu, X., Peng, S., Cao, Y.P., Qi, X., Huang, X., Liang, D., Ouyang, W.: Unidream: Unifying diffusion priors for relightable text-to-3d generation. arXiv preprint arXiv:2312.08754 (2023) [2](#)
19. Long, X., Guo, Y.C., Lin, C., Liu, Y., Dou, Z., Liu, L., Ma, Y., Zhang, S.H., Habermann, M., Theobalt, C., et al.: Wonder3d: Single image to 3d using cross-domain diffusion. arXiv preprint arXiv:2310.15008 (2023) [2](#), [3](#), [4](#), [7](#)
20. Melas-Kyriazi, L., Laina, I., Rupprecht, C., Neverova, N., Vedaldi, A., Gafni, O., Kokkinos, F.: Im-3d: Iterative multiview diffusion and reconstruction for high-quality 3d generation. arXiv preprint arXiv:2402.08682 (2024) [2](#), [4](#)
21. Melas-Kyriazi, L., Laina, I., Rupprecht, C., Vedaldi, A.: Realfusion: 360deg reconstruction of any object from a single image. In: Proceedings of the IEEE/CVF Conference on Computer Vision and Pattern Recognition. pp. 8446–8455 (2023) [18](#), [19](#)
22. Meng, C., He, Y., Song, Y., Song, J., Wu, J., Zhu, J.Y., Ermon, S.: Sdedit: Guided image synthesis and editing with stochastic differential equations. arXiv preprint arXiv:2108.01073 (2021) [9](#)
23. Mou, C., Wang, X., Xie, L., Wu, Y., Zhang, J., Qi, Z., Shan, Y., Qie, X.: T2i-adapter: Learning adapters to dig out more controllable ability for text-to-image diffusion models. arXiv preprint arXiv:2302.08453 (2023) [5](#)
24. Müller, T., Evans, A., Schied, C., Keller, A.: Instant neural graphics primitives with a multiresolution hash encoding. ACM Transactions on Graphics (ToG) **41**(4), 1–15 (2022) [4](#), [9](#)
25. Poole, B., Jain, A., Barron, J.T., Mildenhall, B.: Dreamfusion: Text-to-3d using 2d diffusion. arXiv preprint arXiv:2209.14988 (2022) [4](#), [9](#), [18](#)
26. Qian, G., Mai, J., Hamdi, A., Ren, J., Siarohin, A., Li, B., Lee, H.Y., Skorokhodov, I., Wonka, P., Tulyakov, S., et al.: Magic123: One image to high-quality 3d object generation using both 2d and 3d diffusion priors. arXiv preprint arXiv:2306.17843 (2023) [2](#), [4](#), [12](#), [18](#)
27. Radford, A., Kim, J.W., Hallacy, C., Ramesh, A., Goh, G., Agarwal, S., Sastry, G., Askell, A., Mishkin, P., Clark, J., et al.: Learning transferable visual models from natural language supervision. In: International conference on machine learning. pp. 8748–8763. PMLR (2021) [5](#), [9](#), [12](#), [18](#)
28. Salimans, T., Goodfellow, I., Zaremba, W., Cheung, V., Radford, A., Chen, X.: Improved techniques for training gans. Advances in neural information processing systems **29** (2016) [12](#)
29. Schuhmann, C., Beaumont, R., Vencu, R., Gordon, C., Wightman, R., Cherti, M., Coombes, T., Katta, A., Mullis, C., Wortsman, M., et al.: Laion-5b: An open large-scale dataset for training next generation image-text models. Advances in Neural Information Processing Systems **35**, 25278–25294 (2022) [4](#)

30. Shi, R., Chen, H., Zhang, Z., Liu, M., Xu, C., Wei, X., Chen, L., Zeng, C., Su, H.: Zero123++: a single image to consistent multi-view diffusion base model. arXiv preprint arXiv:2310.15110 (2023) [2](#), [4](#), [6](#)
31. Shi, Y., Wang, P., Ye, J., Long, M., Li, K., Yang, X.: Mvdream: Multi-view diffusion for 3d generation. arXiv preprint arXiv:2308.16512 (2023) [3](#), [7](#), [9](#), [10](#), [18](#)
32. Sohl-Dickstein, J., Weiss, E., Maheswaranathan, N., Ganguli, S.: Deep unsupervised learning using nonequilibrium thermodynamics. In: International conference on machine learning. pp. 2256–2265. PMLR (2015) [4](#)
33. Tang, J., Chen, Z., Chen, X., Wang, T., Zeng, G., Liu, Z.: Lgm: Large multi-view gaussian model for high-resolution 3d content creation. arXiv preprint arXiv:2402.05054 (2024) [8](#)
34. Wang, P., Shi, Y.: Imagedream: Image-prompt multi-view diffusion for 3d generation. arXiv preprint arXiv:2312.02201 (2023) [3](#), [5](#), [7](#), [9](#), [10](#), [11](#), [12](#), [18](#)
35. Wang, Z., Lu, C., Wang, Y., Bao, F., Li, C., Su, H., Zhu, J.: Prolificdreamer: High-fidelity and diverse text-to-3d generation with variational score distillation. Advances in Neural Information Processing Systems **36** (2024) [4](#), [9](#)
36. Wang, Z., Bovik, A.C., Sheikh, H.R., Simoncelli, E.P.: Image quality assessment: from error visibility to structural similarity. IEEE transactions on image processing **13**(4), 600–612 (2004) [18](#), [19](#)
37. Wei, J., Wang, H., Feng, J., Lin, G., Yap, K.H.: Taps3d: Text-guided 3d textured shape generation from pseudo supervision. In: Proceedings of the IEEE/CVF Conference on Computer Vision and Pattern Recognition. pp. 16805–16815 (2023) [4](#)
38. Yang, G., Huang, X., Hao, Z., Liu, M.Y., Belongie, S., Hariharan, B.: Pointflow: 3d point cloud generation with continuous normalizing flows. In: Proceedings of the IEEE/CVF international conference on computer vision. pp. 4541–4550 (2019) [4](#)
39. Yang, X., Chen, Y., Chen, C., Zhang, C., Xu, Y., Yang, X., Liu, F., Lin, G.: Learn to optimize denoising scores for 3d generation: A unified and improved diffusion prior on nerf and 3d gaussian splatting. arXiv preprint arXiv:2312.04820 (2023) [4](#)
40. Ye, H., Zhang, J., Liu, S., Han, X., Yang, W.: Ip-adapter: Text compatible image prompt adapter for text-to-image diffusion models. arXiv preprint arXiv:2308.06721 (2023) [5](#), [7](#)
41. Ye, J., Wang, P., Li, K., Shi, Y., Wang, H.: Consistent-1-to-3: Consistent image to 3d view synthesis via geometry-aware diffusion models. arXiv preprint arXiv:2310.03020 (2023) [2](#), [4](#)
42. Zhang, R., Isola, P., Efros, A.A., Shechtman, E., Wang, O.: The unreasonable effectiveness of deep features as a perceptual metric. In: Proceedings of the IEEE conference on computer vision and pattern recognition. pp. 586–595 (2018) [18](#), [19](#)

A Appendix

In this Appendix, we provide additional implementation details in Appendix A.1, evaluation on the novel view synthesis in Appendix A.2, additional qualitative comparisons in Appendix A.3. We present limitations and future work in Appendix A.4.

A.1 Additional Implementation Details.

Network Structure. We build our network on the Stable Diffusion backbone, while we make several changes on the structure: 1) We incorporate a frozen CLIP pre-trained Vision Transformer [27] as global feature extractor. 2) We adopt the same denoising U-Net with shared weights to extract local features at fixed time step 0. 3) We extend the original 2D self attention layer into 3D by concatenating keys and values from different views to facilitate information propagation. 4) We encode the camera pose with a two layer MLP, which is then added to time embedding as residuals. The proposed control label is embedded and added to the time embedding in the same way.

SDS Optimization. We use the implicit volume implementation in threestudio [8] as our 3D representation, which includes a multi-resolution hash-grid and a MLP to predict density and RGB. For camera views, we sample the camera in exactly the same way as how we render the 3D dataset. To optimize the coarse generation results, we first convert the generated mesh from Instant3D into the implicit volume by randomly rendering and distilling the appearance and occupancy of the mesh with L1 loss. We set the the total steps for this stage to be 1000, which takes about 1 min. After this initialization stage, we optimize the implicit volume utilizing SDS loss with a small range of denoising timestep as [0.02, 0.5]. The optimization process takes about 15min with 2500 steps. The update interval for the proposed Anchor Iterative Update loss is set to be 500 and the control label is set to 1 for the first input view and 0.5 for the other three input views in our experiments. Similar as prior arts [21, 26], we adopt a l1 loss from the first input view to further refine the details in the generation results. In both stages, we adopt Adam optimizer and adopt the orientation loss [25] to enhance the performance.

Instant3D Implementation. We reproduce Instant3D [14] following the published paper while making several minor changes: 1) We adopt ImageDream [34] and MVDream [31] as the multi-view diffusion models at the first stage to generate four multi-view images from single-image and text prompt, respectively. 2) We implement the sparse-view large reconstruction model strictly follow the original paper while training it on the same dataset as the proposed Magic-Boost method. The whole training procedure takes about 7 days on 32 A100 GPUs.

A.2 Evaluation on Novel View Synthesis.

We employ PSNR, SSIM [36], LPIPS [42] to evaluate the performance of our model on novel view synthesis task on the Google Scanned Dataset (GSO) [6]. In

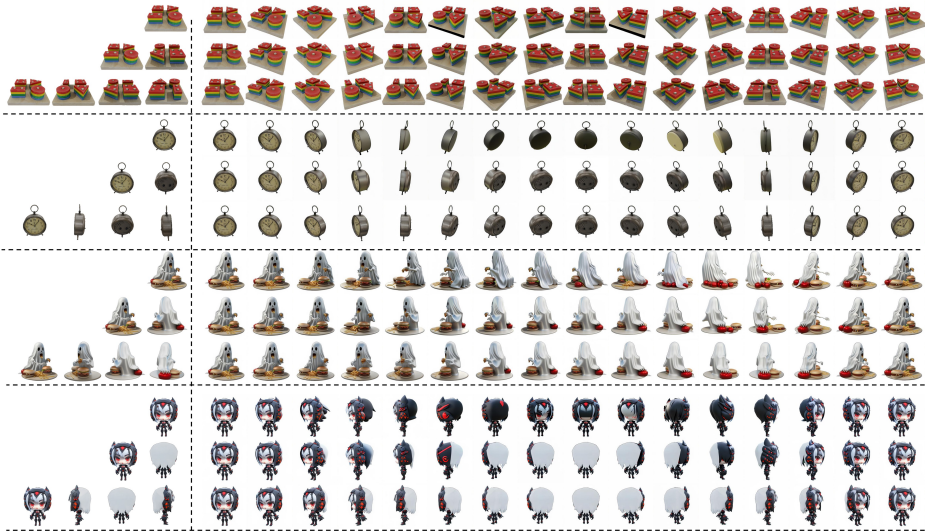


Fig. 9: Effects of using different condition views as input. Left column shows the input multi-view images and the right column shows synthesized novel views.

Table 2: Quantitative Comparisons in Novel view synthesis. We report PSNR, SSIM [36], LPIPS [42] on the GSO [6] dataset.

Model	Ref Views	PSNR \uparrow	SSIM \uparrow	LPIPS \downarrow
Realfusion [21]	1	15.26	0.722	0.283
Zero123 [16]	1	18.93	0.779	0.166
Syncdreamer [17]	1	20.05	0.798	0.146
Ours	1	19.31	0.802	0.165
Ours	2	21.29	0.828	0.137
Ours	4	23.98	0.862	0.105

details, we use the same 30 objects chosen by SyncDreamer [17] and render 16 views with uniformly distributed camera poses and environment lighting for each object. To ensure a fair and efficient evaluation process, the first render view is selected as the input image for each baseline and our methods. For multi-view inputs of our method, we select views orthogonal to the first input view. As shown in Tab. 2, benefit from the more comprehensive information provided by multi-view inputs, our model significantly outperforms previous methods that rely on only single-view image as input and synthesize novel views with much higher fidelity. We provide more novel view synthesis results in Fig. 9.

A.3 More Qualitative Results.

We provide more qualitative results in this Section. Fig. 10 and Fig. 11 shows more results of our Image-to-3D generation results. In this Figure, we show from left to right: the input image, the generated multi-view images, the coarse output from Instant3D and the boosted results of our method. In Fig. 12 and Fig. 13, we show results of text-to-3D generation. In text-to-3D setting, we directly generates the multi-view images from the given text input. In Fig. 12 and Fig. 13. from left to right, we show the input text, the generated multi-view images, the coarse output and the boosted results of our method. In Fig. 14, we show more qualitative comparisons of our method with other possible boost method, including using Stable Diffusion to boost the results (Sd-boost) and using Zero123-XL [16] to boost the results (image-boost). As shown in Fig. 14, our model provides more precise SDS guidance which can effectively maintain the identity and enhance local details in both geometry and texture of initial generation results. We also illustrate the effects of the control label in Fig. 15, while using high control strength the model highly rely on the consistency of the input multi-view images, leading to chaotic texture in the inconsistent regions. When we reduce the control strength of the back view here, the model generates smoother results with better visual quality.

A.4 Failure Cases.

The use of pseudo 3D multi-view images synthesized by the finetined 2D multi-view diffusion model as inputs imposes an unavoidable influence on our model’s performance. Despite implementing data augmentation during training to emulate 3D inconsistencies and attempting to bridge the domain gap, this approach still results in inaccuracies for faulty structures. For instance, as shown in Fig. 16, the model fails to generated correct results on the tail of the horse due to the seriously 3D inconsistent on the generated multi-view images. Exploring 2D multi-view diffusion models with better generation quality would further improve our model’s performance.

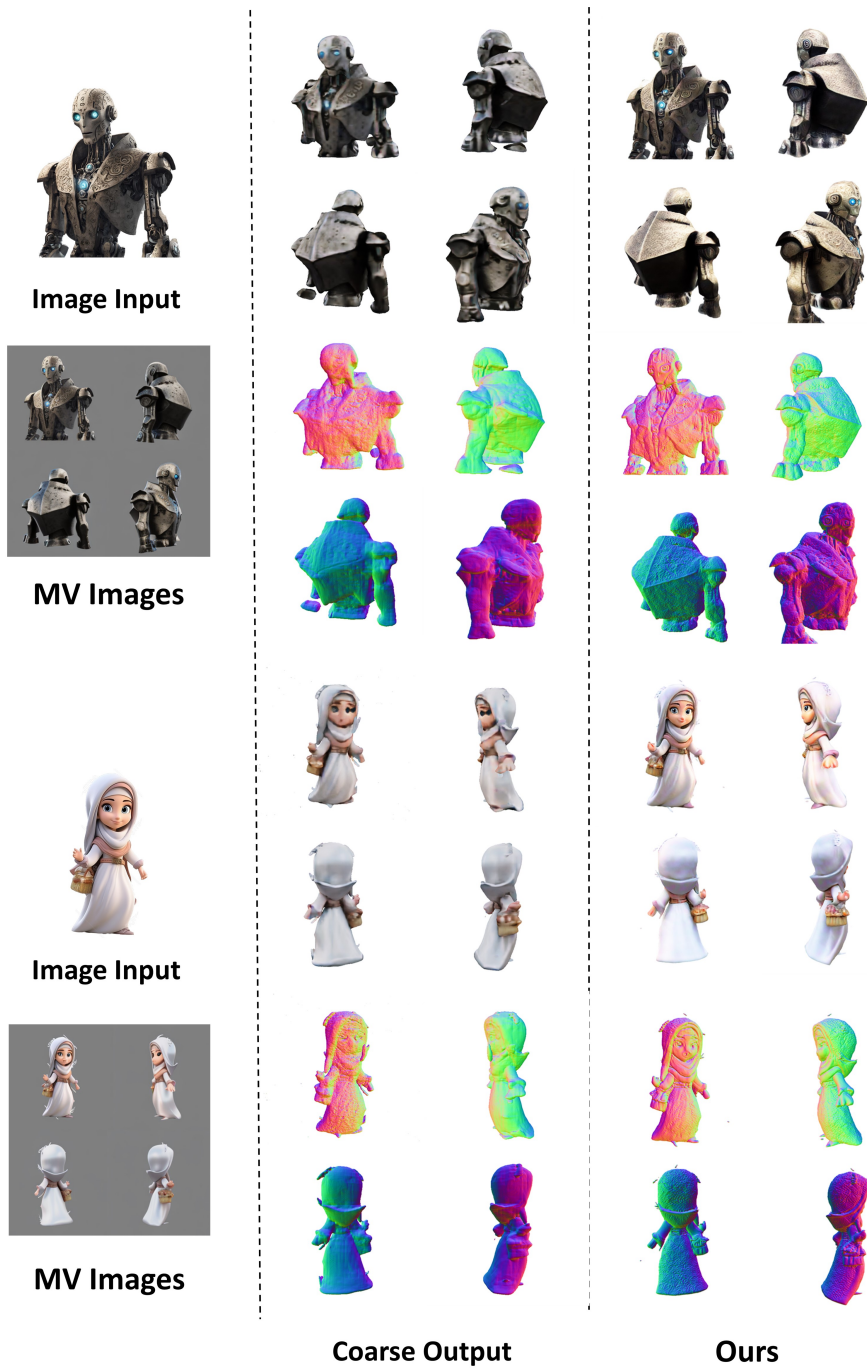


Fig. 10: More results of Image conditioned generation. From left to right: the input image, the generated multi-view images, the coarse output from Instant3D and the boosted results of our method.

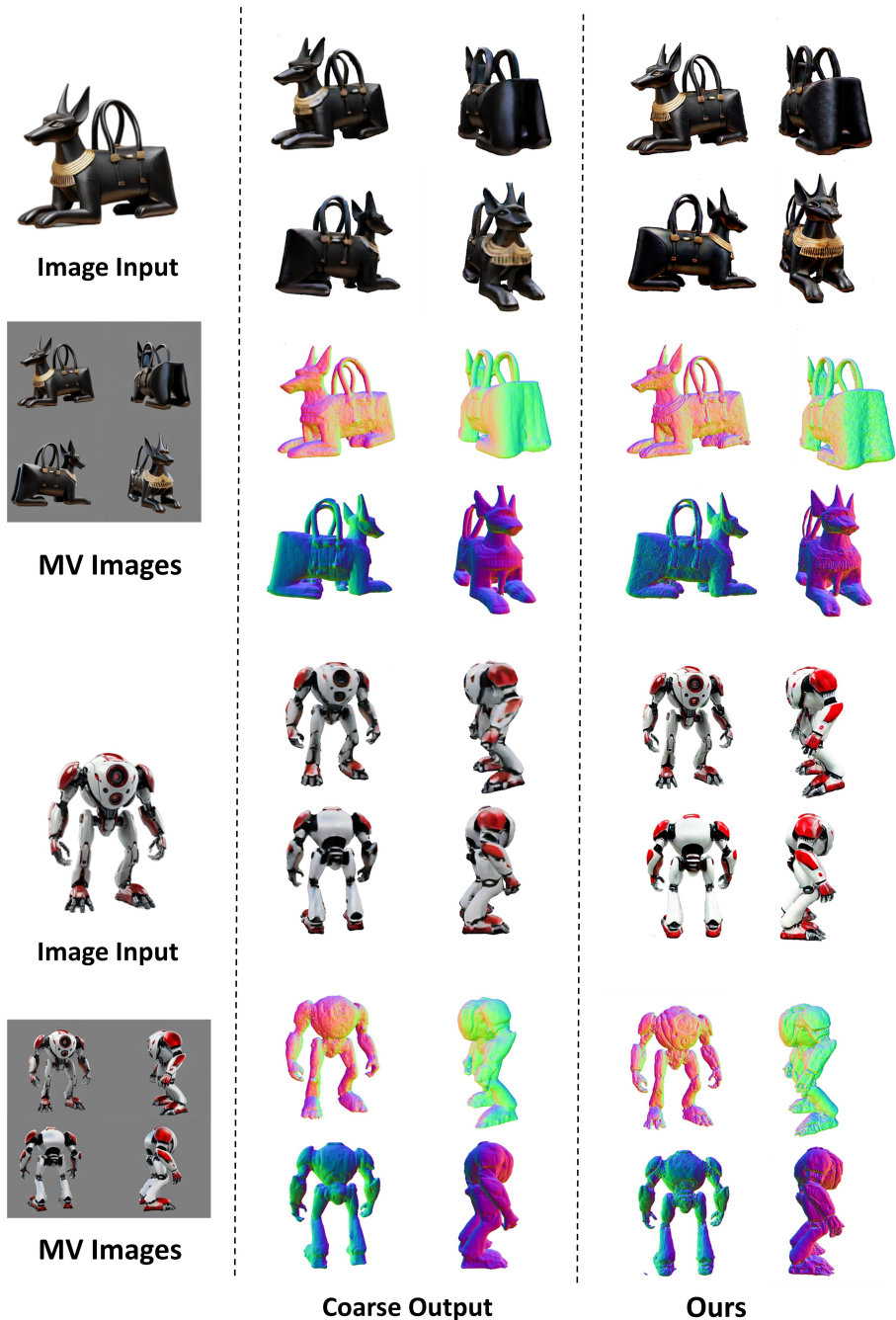


Fig. 11: More results of Image conditioned generation. From left to right: the input image, the generated multi-view images, the coarse output from Instant3D and the boosted results of our method.

Wreath made of multicolored spring flower.

Text Input



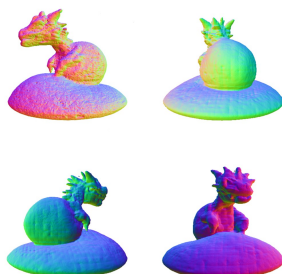
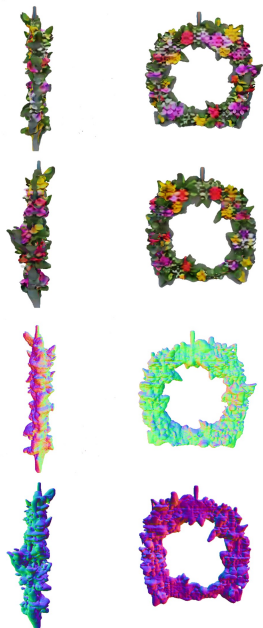
MV Images

A baby Dragon hatching out on a stone egg.

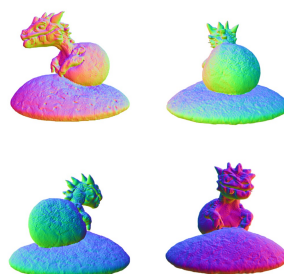
Text Input



MV Images



Coarse Output



Ours

Fig. 12: More results of text conditioned generation. From left to right, we show the input text, the generated multi-view images, the coarse output and the boosted results of our method.

An old fashioned pilots leather cap.

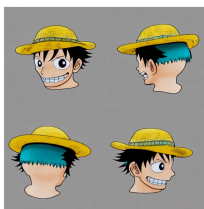
Text Input



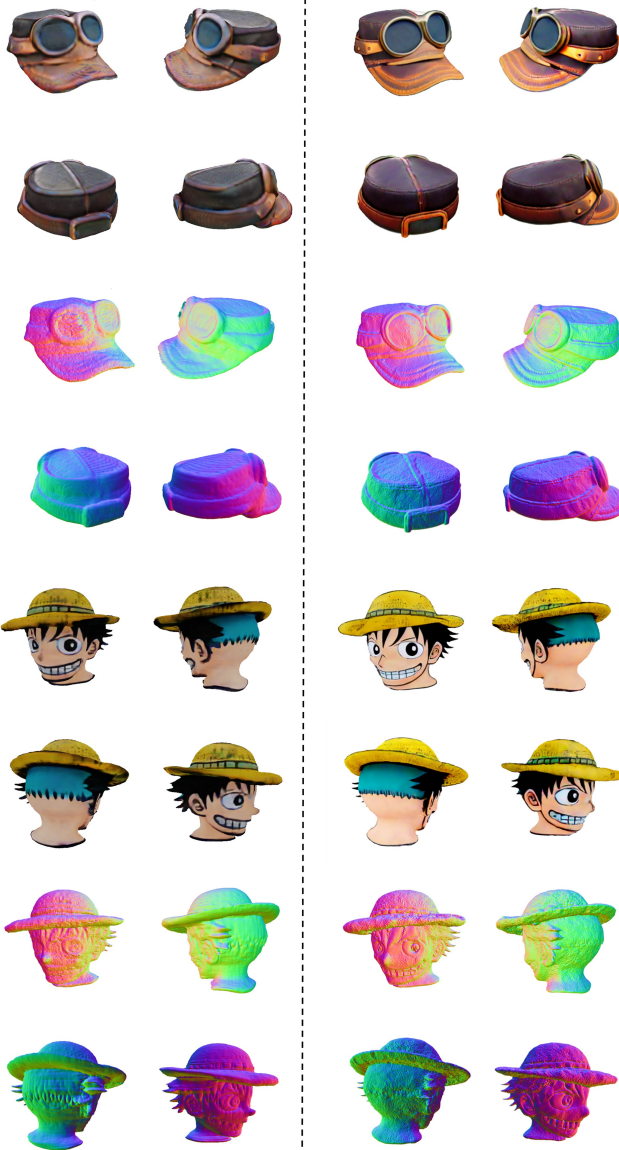
MV Images

Luffy from one piece cute render head.

Text Input



MV Images



Coarse Output

Ours

Fig. 13: More results of text conditioned generation. From left to right, we show the input text, the generated multi-view images, the coarse output and the boosted results of our method.



Fig. 14: More comparison results of our boost method with ours, including sd-boost (Stable Diffusion) and image-boost (Zero123-XL [16]). As shown in the figure, our model can effectively maintain the identity and enhance local details in both geometry and texture of coarse generation results.

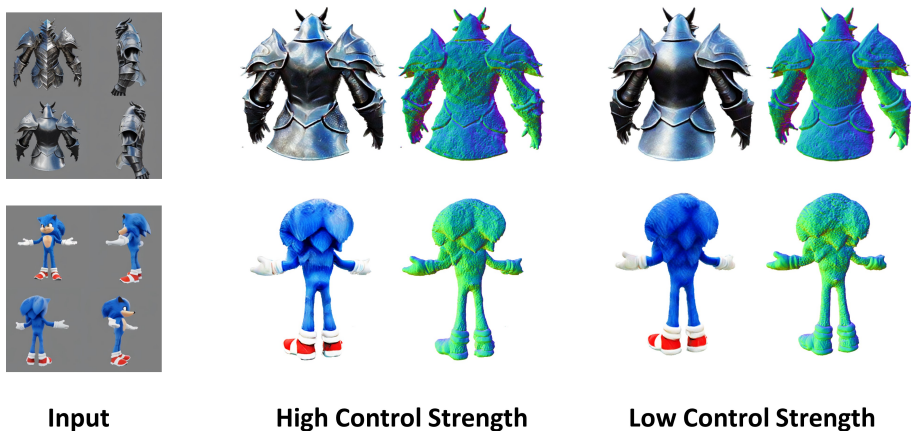


Fig. 15: Illustration of the effects of control label. While using high control strength the model highly rely on the consistency of the input multi-view images, leading to chaotic texture in the inconsistent regions. When we reduce the control strength of the back view here, the model generates smoother results with better visual quality.

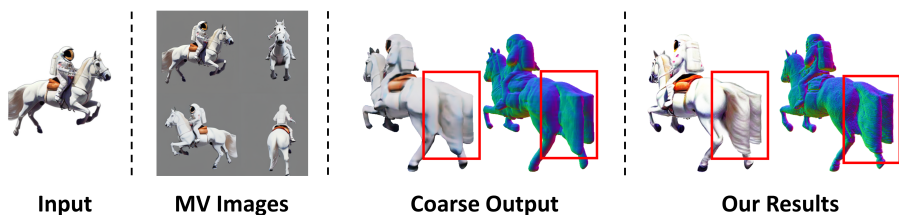


Fig. 16: Illustration of a failure case. the model fails to generated correct results on the tail of the horse due to the seriously 3D inconsistent on the generated multi-view images. Exploring 2D multi-view diffusion models with better generation quality would further improve our model's performance.